

IRRADIATION-INDUCED PRECIPITATION AND MECHANICAL PROPERTIES OF VANADIUM ALLOYS AT <430°C, H. M. Chung, J. Gazda, and D. L. Smith (Argonne National Laboratory)

OBJECTIVE

The objective of this study is to identify dense irradiation-induced precipitation of very fine particles that causes severe dislocation channeling and poor work-hardening capability in V-4Cr-4Ti at <430°C.

ABSTRACT

Recent attention to V-base alloys has focused on the effect of low-temperature (<430°C) irradiation on tensile and impact properties of V-4Cr-4Ti. In previous studies, dislocation channeling, which causes flow localization and severe loss of work-hardening capability, has been attributed to dense, irradiation-induced precipitation of very fine particles. However, efforts to identify the precipitates were unsuccessful until now. In this study, analysis by transmission electron microscopy (TEM) was conducted on unalloyed V, V-5Ti, V-3Ti-1Si, and V-4Cr-4Ti specimens that were irradiated at <430°C in conventional and dynamic helium charging experiments. By means of dark-field imaging and selected-area-diffraction analysis, the characteristic precipitates were identified to be $(V,Ti_{1-x})(C,O,N)$. Evidence indicates that severe dislocation channeling and poor work-hardening capability in V-4Cr-4Ti occur at <430°C as a result of dense precipitation of $(V,Ti_{1-x})(C,O,N)$. In V-3Ti-1Si, precipitation of $(V,Ti_{1-x})(C,O,N)$ was negligible at <430°C, and as a result, dislocation channeling did not occur and work-hardening capability was high.

INTRODUCTION

Recently, attention to vanadium alloy development for fusion reactor application has focused on the performance of V-(4-5)Cr-(4-5)Ti after low-temperature irradiation; tensile¹⁻⁷ and impact^{4,6,7} properties after irradiation at <430°C have been of special interests. It has been reported that a 500-kg heat (832665) and a 30-kg heat BL-47 of V-4Cr-4Ti and a 80-kg heat BL-63 of V-5Cr-5Ti exhibited low uniform elongation as a result of virtual loss of work-hardening capability after irradiation at 80-430°C in several fission-reactor experiments, i.e., in HFBR,¹ HFIR,^{2,3} EBR-II X530,^{4,5} ATR,⁶ FFTF MOTA,⁷ and FFTF COBRA-1A2⁷ experiments. In contrast to the tensile behavior at <430°C, V-Cr-Ti, V-Ti, and V-Ti-Si alloys exhibited generally good work-hardening capability after irradiation at $\geq 500^\circ\text{C}$.⁸ The 500-kg heat of V-4Cr-4Ti also exhibited poor impact properties after irradiation at $\leq 390^\circ\text{C}$.^{4,6,7} This was surprising, in view of a previous report that the 30-kg heat of V-4Cr-4Ti exhibited good impact properties after irradiation at $\geq 430^\circ\text{C}$ in the FFTF,⁹ and that the 500-kg heat exhibited excellent impact properties in the nonirradiated state.⁸ In subsequent studies of the tensile behavior of the 500-kg heat, the poor work-hardening capability was found to be due to dislocation channeling that occurred extensively in the alloy after irradiation at $\leq 390^\circ\text{C}$.¹⁰⁻¹² Furthermore in these studies, severe dislocation channeling was attributed to dense precipitation of very fine particles (<10 nm in size) during irradiation at the low temperatures.¹⁰⁻¹² Therefore, identification of the irradiation-induced precipitates and understanding the mechanism of dislocation channeling have been of major importance in understanding the irradiation performance of V alloys at <430°C. However, initial efforts to gain information on the composition of the very fine precipitates by electron energy loss spectroscopy were inconclusive.^{11,12}

In this work, TEM selected-area-diffraction (SAD) analysis and dark-field imaging techniques were utilized to identify the very fine irradiation-induced precipitates in the 500-kg heat of V-4Cr-4Ti that was irradiated in an Li environment in the EBR-II at $\approx 390^\circ\text{C}$, and in laboratory heats of V, V-5Ti, V-3Ti-1Si, and V-4Cr-4Ti (BL-47) that were irradiated at ≈ 420 - 600°C in the dynamic helium charging experiment (DHCE) in the FFTF.^{8,13} In contrast to the poor work-hardening capability of the large-scale and laboratory heats of V-4Cr-4Ti irradiated in the conventional irradiation experiments (i.e., non-DHCE) at ≈ 390 and $\approx 430^\circ\text{C}$, respectively, work-

hardening capabilities of the laboratory heats of V-4Cr-4Ti and V-3Ti-1Si were significantly higher after irradiation in the DHCE at $\approx 430^\circ\text{C}$. This variation in work-hardening capability is manifested by significant variation in uniform elongation as shown in Fig. 1.7 Therefore, of particular interest in this study was not only identification of the irradiation-induced precipitates but also relationship among degree of precipitation, dislocation channeling, and work-hardening capability of several alloys that were irradiated at $<430^\circ\text{C}$.

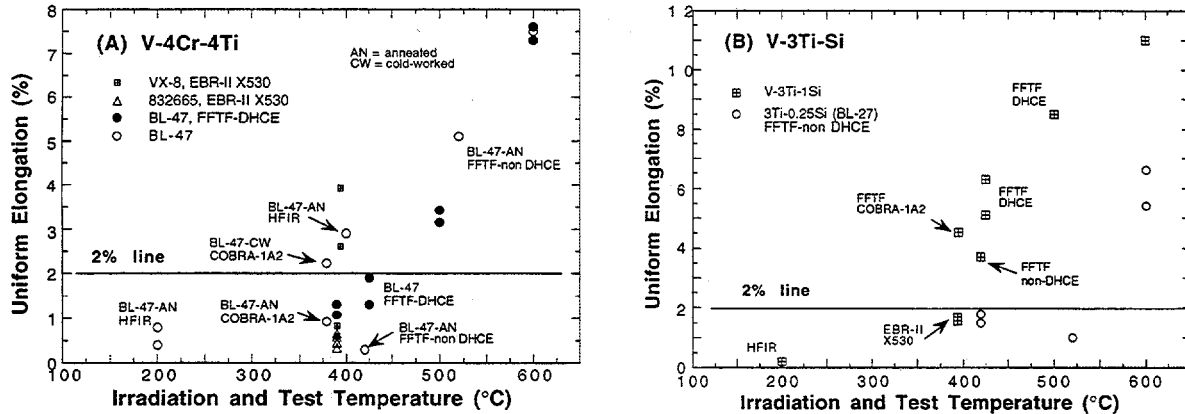


Fig. 1. Uniform elongation as a function of irradiation temperature (same as test temperature) of V-4Cr-4Ti (A) and V-3Ti-1Si (B), showing significant variation in work-hardening capability, depending on heat and irradiation condition.

EXPERIMENTAL PROCEDURES

The elemental composition of the alloys investigated in this study, determined prior to irradiation, is given in Table 1. TEM analysis was not conducted on Heat VX-8 (V-3.7Cr-3.9Ti; O, 350 wppm; N, 70; C, 300; Si, 500; Nb, 1280; Al, 1120; Co, 500; Fe, 280; Mo, 270; and Zr, 19 wppm) and Heat BL-27 (V-3.1Ti-0.25Si; O, 210; N, 310; and C, 310 wppm), although uniform elongation of the heats was relatively high, as shown in Fig. 1. Details of conventional and DHCE irradiation experiments, in which TEM disks and tensile specimens of these alloys were irradiated, are summarized in Table 2. TEM disks and tensile specimens were machined out of cold-worked sheets ≈ 0.3 and ≈ 1 mm thick, respectively, followed by annealing at 1050 – 1125°C for 1 h in ion-pumped vacuum. The irradiated specimens were then retrieved from the irradiation capsules, and Li that was bonded onto the specimens was cleaned off in a bath of liquid ammonia. Then, the specimens were further cleaned ultrasonically in a bath of ethyl alcohol. TEM disks were also prepared out of the gage area of broken tensile specimens. All TEM disks were jet-thinned at -10°C in a solution of 15% sulfuric acid, 72% methanol, and 13% butyl cellulose. TEM was conducted with a JEOL 100CX-II scanning transmission electron microscope (100 keV) or with a Philips CM-30 analytical electron microscope (300 keV).

Table 1. Chemical composition of vanadium alloys

Heat ID	Nominal Comp. (wt.%)	Impurity Concentration (wt. ppm)			
		O	N	C	Si
BL-19 ^a	V	1101	161	360	—
BL-46 ^a	4.6Ti	305	53	85	160
BL-45 ^a	2.5Ti-1Si	345	125	90	9900
BL-47 ^b	4.1Cr-4.3Ti	350	220	200	870
832665 ^c	3.8Cr-3.9Ti	310	85	80	783

^a15-kg laboratory heat

^b30-kg laboratory heat

^c500-kg production-scale heat

RESULTS

A typical bright-field image of dislocation channels, shown in Fig. 2, was obtained from the 500-kg Heat 832665 of V-4Cr-4Ti that was irradiated to ≈ 4 dpa and tensile-tested at 390°C. Several SAD patterns were obtained from the precipitate-rich regions, such as those in Fig. 2, in one orientation, e.g., (110) zone of the matrix. Using reflections from the precipitates, we obtained many dark-field images in this orientation. Then, the specimen was tilted to several

Table 2. Summary of conditions under which TEM disks and tensile specimens were irradiated

Alloy Type	Alloy Heat	Irradiation	Environment	Temperature (°C)	dpa
V-4Cr-4Ti	832665	EBR-II X530	Li	≈ 390	4
V	BL-19	FFTF-DHCE	Li	430-600	13-27
V-5Ti	BL-46	FFTF-DHCE	Li	430-600	13-27
V-3Ti-1Si	BL-45	FFTF-DHCE	Li	430-600	13-27
V-4Cr-4Ti	BL-47	FFTF-DHCE	Li	430-600	13-27

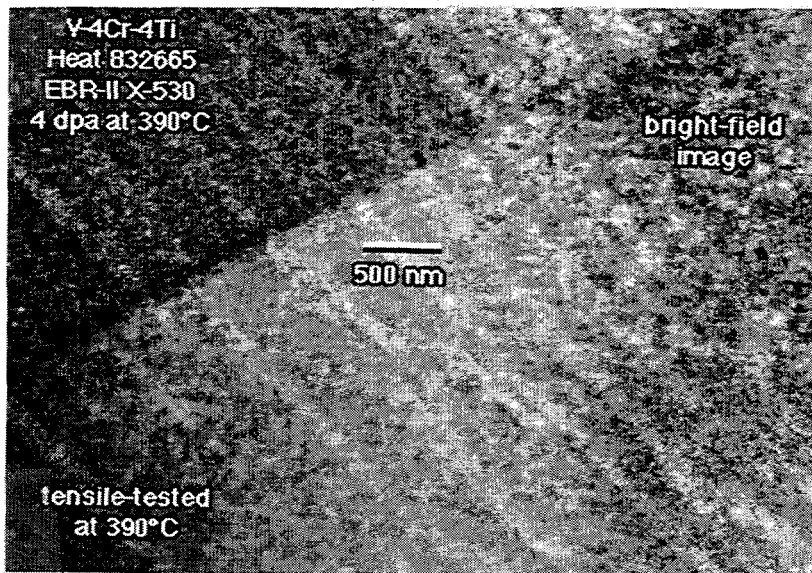


Fig. 2.

Bright-field image of dislocation channels in 500-kg V-4Cr-4Ti Heat 832665 tensile specimen irradiated to ≈ 4 dpa at 390°C in EBR-II X530 experiment and tensile-tested at 390°C

other orientations, e.g., (100), (120), and (310) zones of the matrix, and more SAD patterns and dark-field images of the precipitates were obtained at the new orientation. Because Heat 832665 V-4Cr-4Ti specimens that were irradiated at $\approx 390^\circ\text{C}$ in the EBR-II X530 experiment contained a significantly high volume fraction of the precipitates,¹¹ dark-field images of the unknown precipitates could be obtained without much difficulty. Typical examples of SAD patterns are shown in Figs. 3-5, which correspond, respectively, to the (110), (310), and (320) zones of the matrix. For most SAD patterns, many double-diffraction spots are present, and, at the same time, precipitate reflections are superimposed on most matrix reflections. As a result, "pure" matrix reflections were difficult to find. Because of these two factors, significant difficulty was commonly encountered in isolating and identifying the operating precipitate zone in a given SAD pattern.

A typical example of a dark-field image of the precipitates, observed in a TEM disk of the 500-kg V-4Cr-4Ti heat after irradiation to ≈ 4 dpa at $\approx 390^\circ\text{C}$ in the EBR-II, is given in Fig. 6. Very fine (size 3-10 nm), dense precipitates are visible; number density and volume fraction of precipitates in the figure correspond to $\approx 3.5 \times 10^{17} \text{ cm}^{-3}$ and $\approx 1.2\%$, respectively.

The SAD pattern in Fig. 3 shows numerous double-diffraction spots and precipitate reflections that correspond to the (111) zone of an fcc structure that is parallel to the (110) zone of the bcc matrix. Exactly the same orientational relationship was observed for relatively larger

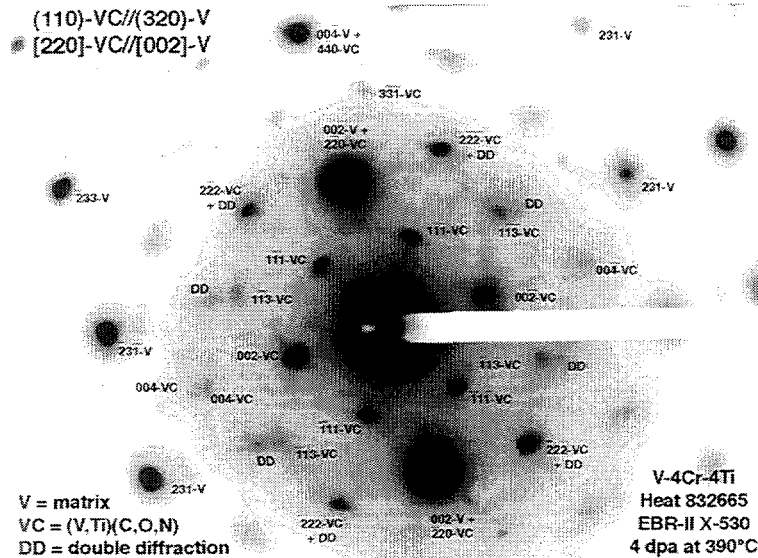


Fig. 5.

SAD pattern from V-4Cr-4Ti Heat 832665 TEM disk irradiated to ≈ 4 dpa at 390°C in EBR-II X530, showing (110) zone of $(V,Ti_{1-x})(C,O,N)$ precipitates nearly parallel to (320) zone of matrix. Letters V, VC, and DD denote, respectively, matrix, $(V,Ti_{1-x})(C,O,N)$, and double diffraction.

irradiation-induced precipitates is indicated only by the streaks, and dark-field images could be obtained only with the streaks that are visible near the matrix reflections. Such streaks are absent in the (100) zone of V-3Ti-1Si irradiated in the FFTF-DHCE to ≈ 27 dpa at $\approx 430^\circ\text{C}$ (Fig. 10), indicating that precipitation in this alloy was insignificant under the irradiation conditions.

Initially, it was suspected that the characteristic precipitates could be either irradiation-enhanced precipitates of α -Ti (hcp, $a_0 = 0.29504$ nm, $c_0 = 0.46833$ nm), Ti_2O (hcp, $a_0 = 0.2959$ nm, $c_0 = 0.4845$ nm), Ti_3O (hcp, $a_0 = 0.4991$ nm, $c_0 = 0.2879$ nm), or metastable ω -phase (hcp, $a_0 = 0.4573$ - 0.4598 nm, $c_0 = 0.2804$ - 0.2818 nm). A Ti-rich Ti-V phase has been observed in Ti-V alloys by several investigators.^{14,15} However, the diffraction behavior, such as that manifested in the SAD patterns in Figs. 2-4 and 6-9, was not consistent with any of these systems. Of particular importance is fact that the characteristic precipitates that exhibit the same diffraction behavior were also observed in unalloyed vanadium (BL-19, Fig. 6). Therefore, we searched for an fcc compound based on V.

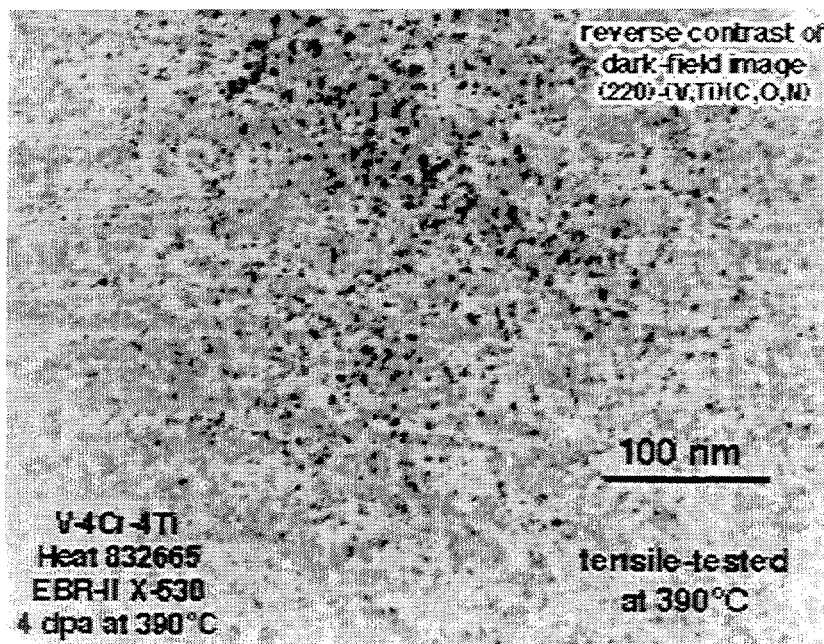


Fig. 6.

Reverse-contrast dark-field image of $(V,Ti_{1-x})(C,O,N)$ precipitates in V-4Cr-4Ti Heat 832665 TEM disk irradiated to ≈ 4 dpa at 390°C in EBR-II X530 experiment.

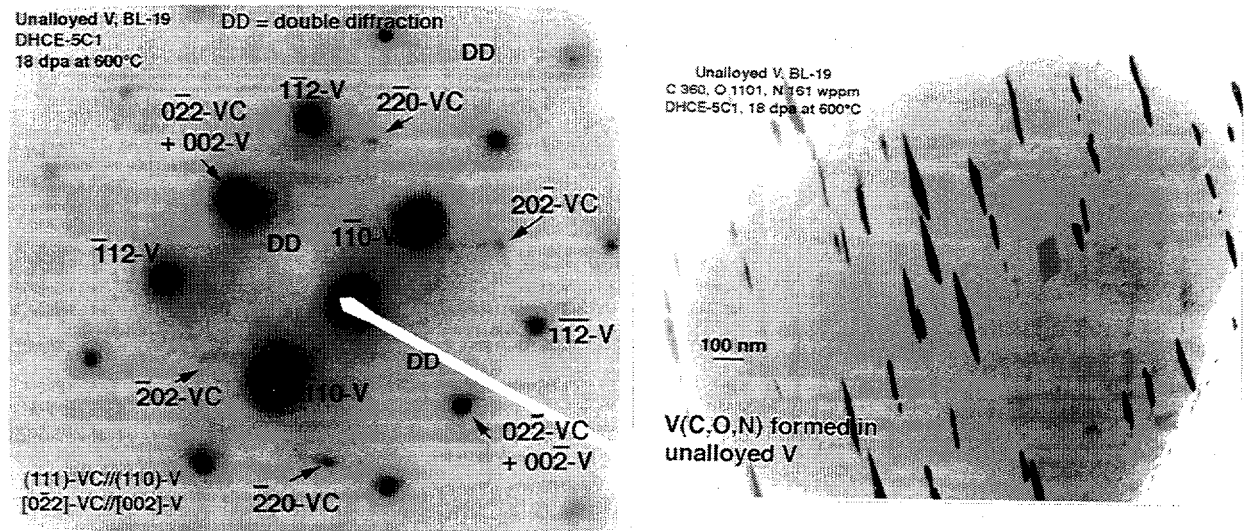


Fig. 7. SAD pattern (left) and reverse-contrast dark-field image (right) of $V(C,O,N)$ precipitates observed in unalloyed V Heat BL-19 TEM disk irradiated to ≈ 18 dpa at 600°C in FFTE-DHCE, showing (111) zone of precipitate parallel to (110) zone of matrix. Letters V, VC, and DD denote, respectively, matrix, $V(C,O,N)$, and double diffraction spots.

The SAD patterns shown in Figs. 3-5 and 7-10 could be indexed precisely only on the basis of the structure of VC, an fcc compound with a lattice constant of $a_0 = 0.4168\text{-}0.4169$ nm.^{16,17} Meanwhile, VO (fcc, $a_0 = 0.409$ nm) and VN (fcc, $a_0 = 0.413$ nm) are isostructural with VC, and lattice constants of the three phases are similar.^{16,17} Considering this and the fact that the three compounds are mutually soluble, we conclude that the precipitates are $V(C,O,N)$, an fcc (NaCl) structure (space group $Fm\bar{3}m$) with a lattice constant $a_0 = 0.415\text{-}0.420$ nm.

This measured lattice spacing is $\approx 1.5\text{-}2.0\%$ smaller than the lattice spacings reported for TiC (fcc, $a_0 = 0.4313\text{-}0.4330$ nm), TiO (fcc, $a_0 = 0.422\text{-}0.425$ nm), or TiN (fcc, $a_0 = 0.4182\text{-}0.4243$ nm).^{16,17} However, this small difference in lattice spacing cannot be discerned conclusively from TEM SAD patterns. Therefore, based on measured lattice spacing alone, it is not possible to conclude whether the precipitates are V- or Ti-based precipitates, i.e., $V(C,O,N)$ or $Ti(C,O,N)$. However, the fact that the characteristic precipitates were observed in unalloyed V (BL-19, Fig. 7) provides conclusive evidence that they are of the $V(C,O,N)$ type. This is supported further by the following observations.

The diffraction characteristics and morphology of the precipitates that formed at higher irradiation temperatures, such as those shown in Figs. 7 (unalloyed V at 600°C), 8 (V-5Ti at 600°C), and 10 (V-3Ti-1Si at 500°C), are essentially the same as the $(V_{0.75}Ti_{0.25})(C,O,N)$ precipitates that were observed in laser and electron-beam welds of V-4Cr-4Ti Heat 832665 after postwelding annealing at 1000°C for 1 h.¹⁸ Kazakov et al. reported that carbides of V (VC or V_2C) were observed in the fusion and heat-affected zones of gas-tungsten-arc welds of V-2.5Zr-0.35C.¹⁹ The morphology of these carbides is essentially the same as that of $V(C,O,N)$ precipitates observed in V, V-5Ti, and V-3Ti-1Si in this study and in the laser and electron-beam welds of Ref. 18. The morphology of V carbides observed by Kazakov et al. in the V-2.5Zr-0.35C welds was in distinct contrast to the spherical morphology of ZrC, which was observed only in the fusion zone of the alloy. Hence, we believe that the irradiation-induced precipitates observed in this study have essentially the fcc (NaCl) structure of VC that is modified in elemental composition; namely, O, and to a lesser extent, N atoms replacing some C atoms and Ti replacing some V in the Ti-containing V alloys.

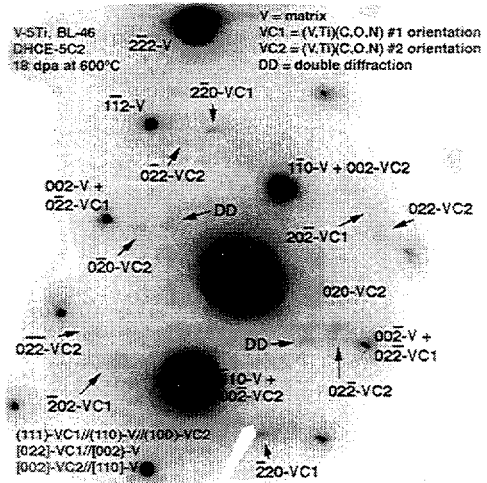
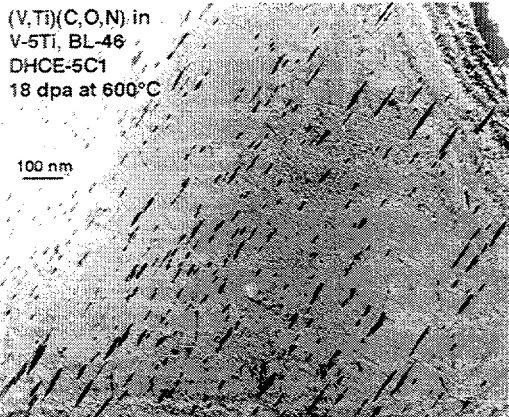
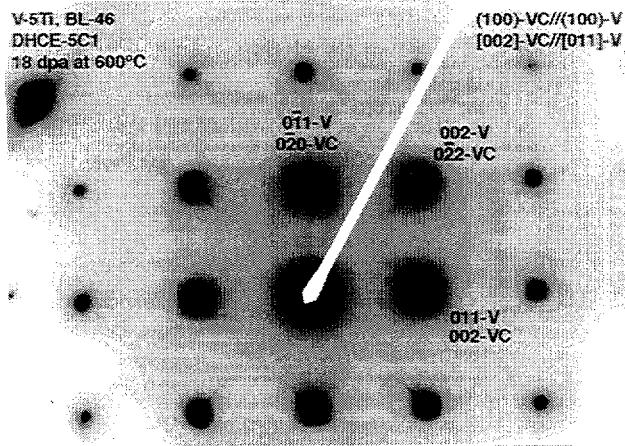
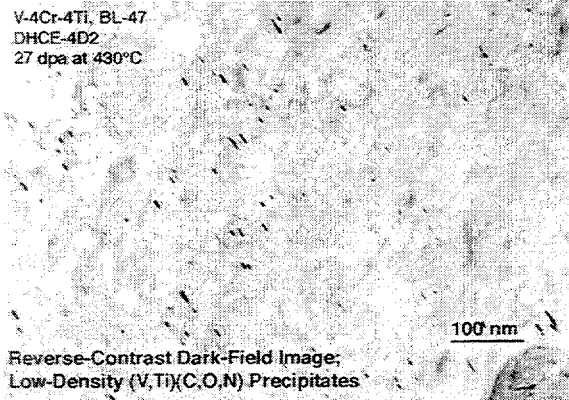
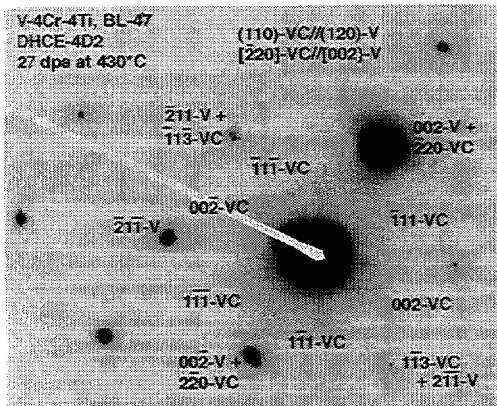


Fig. 8. SAD patterns and reverse-contrast dark-field image of $(V,Ti_{1-x})(C,O,N)$ observed in V-5Ti BL-46 TEM disk irradiated to ≈ 18 dpa at 600°C in FFTF-DHCE. Upper left and right SAD patterns show, respectively, $(100)vc//[(100)v]$ and $(111)vc//[(110)v]$. Letters V, VC, and DD denote, respectively, matrix, $(V,Ti_{1-x})(C,O,N)$, and double diffraction.



Reverse-Contrast Dark-Field Image; Low-Density $(V,Ti)(C,O,N)$ Precipitates

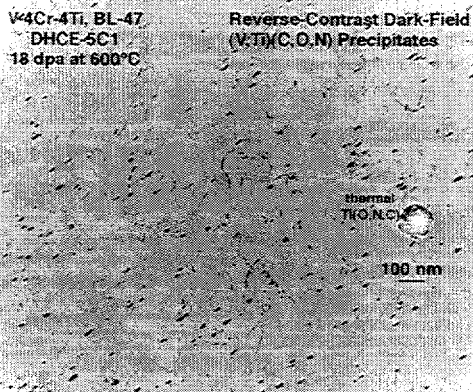


Fig. 9. SAD pattern (top left, ≈ 27 dpa at 430°C) and reverse-contrast dark-field images (top right ≈ 27 dpa at 430°C ; bottom left ≈ 18 dpa at 600°C) of $(V,Ti_{1-x})(C,O,N)$ from V-4Cr-4Ti BL-47 TEM disk irradiated in FFTF-DHCE. The SAD pattern shows $(110)vc//[(120)v]$. Letters V, VC, and DD denote, respectively, matrix, $(V,Ti_{1-x})(C,O,N)$, and double diffraction spots.

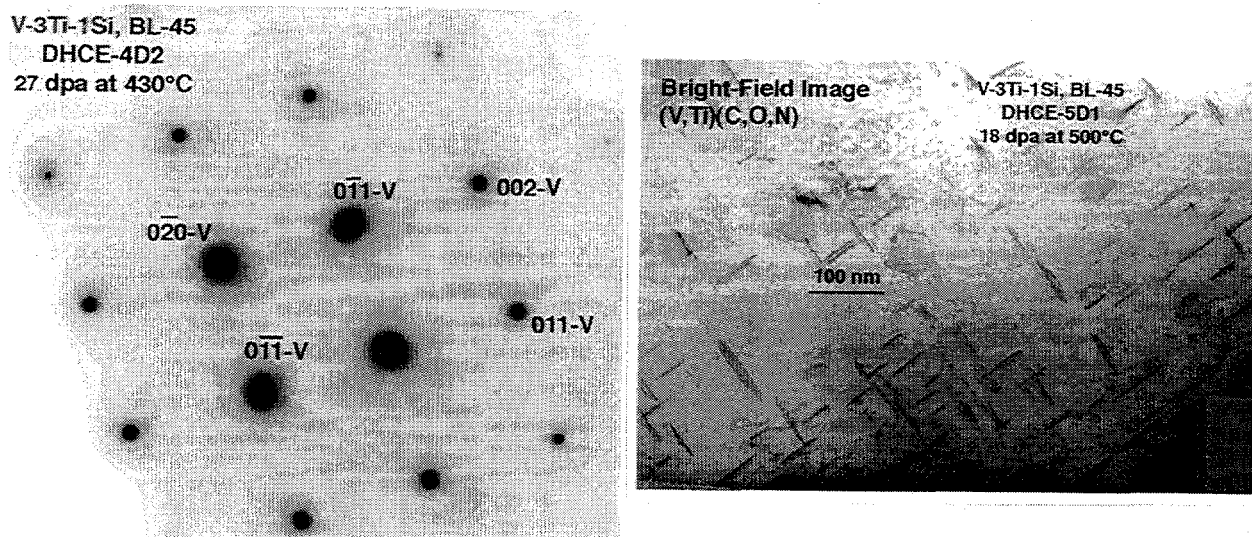


Fig. 10. SAD pattern (TEM disk, ≈ 27 dpa at 430°C) and dark-field image (TEM disk, ≈ 18 dpa at 500°C) of $(\text{V},\text{Ti}_{1-x})(\text{C},\text{O},\text{N})$ precipitates from V-3Ti-1Si BL-45 irradiated in FFTF-DHCE. The SAD pattern shows (100) zone of matrix free of streaks, indicating that $(\text{V},\text{Ti}_{1-x})(\text{C},\text{O},\text{N})$ precipitation at ≈ 27 dpa at 430°C was insignificant.

Thermal $\text{Ti}(\text{O},\text{N},\text{C})$ precipitates form in Ti-containing V alloys during ingot melting and fabrication when combined concentrations of O, N, and C exceed ≈ 400 wppm.²⁰ The morphology of this type of mostly 300-500-nm $\text{Ti}(\text{O},\text{N},\text{C})$ is invariably ellipsoidal or spherical, which is in distinct contrast to the elongated morphology of $\text{V}(\text{C},\text{O},\text{N})$ type precipitates such as those shown in Figs. 7, 8, and 10 in this study and those observed in welds in Refs. 18 and 19. Furthermore, thermally formed $\text{Ti}(\text{O},\text{N},\text{C})$ exhibits an orientational relationship of $(100)_{\text{Ti}(\text{O},\text{N},\text{C})} // (110)_{\text{V}}$.

In contrast to this, the irradiation-induced precipitates of $(\text{V},\text{Ti}_{1-x})(\text{C},\text{O},\text{N})$ analyzed in this study exhibit two orientational relationships, i.e., $(111)_{\text{V}(\text{C},\text{O},\text{N})} // (110)_{\text{V}}$ (Figs. 3, 7, and 9) and $(100)_{\text{V}(\text{C},\text{O},\text{N})} // (100)_{\text{V}}$ (Fig. 8). The latter orientation is identical to the orientation $(110)_{\text{V}(\text{C},\text{O},\text{N})} // (110)_{\text{V}}$ that was observed for the $(\text{V},\text{Ti}_{1-x})(\text{C},\text{O},\text{N})$ precipitated in the welds of the 500-kg V-4Cr-4Ti.¹⁸ The diffraction spots from the very fine $(\text{V},\text{Ti}_{1-x})(\text{C},\text{O},\text{N})$ precipitates in the 500-kg V-4Cr-4Ti specimens, irradiated to ≈ 4 dpa at 390°C , exhibit, as shown in Figs. 4 and 5, streaks in the $\langle 110 \rangle$ and $\langle 111 \rangle$ directions of the precipitate, indicating that they are extremely thin, needlelike precipitates. In contrast to this, the relatively large $(\text{V},\text{Ti}_{1-x})(\text{C},\text{O},\text{N})$ precipitates in V-5Ti, irradiated to ≈ 18 dpa at 600°C , exhibit streaks in the $\langle 110 \rangle$ direction only, showing that they are thin platelets (≈ 10 nm thick and 50-120 nm in diameter).

The diffraction characteristics of $(\text{V},\text{Ti}_{1-x})(\text{C},\text{O},\text{N})$ in the (100) orientation, such as those shown in Fig. 8, are in sharp contrast to those of the irradiation-induced Ti_5Si_3 precipitates at the same matrix orientation.²⁰ For example, diffraction patterns that are characteristic of the latter type of precipitates are shown in Fig. 11 [Ti_5Si_3 on the (100) and (111) zones of the matrix], which was obtained from V-3Ti-1Si (BL-45) irradiated to ≈ 18 dpa at 600°C in the FFTF-DHCE. Although the morphology of the Ti_5Si_3 precipitates shown in the figure is similar to that of thermally formed ellipsoidal $\text{Ti}(\text{O},\text{N},\text{C})$, their diffraction patterns differ from those of $\text{Ti}(\text{C},\text{O},\text{N})$ ²⁰ and $(\text{V},\text{Ti}_{1-x})(\text{C},\text{O},\text{N})$, e.g., those on the (100) zone of the matrix shown in Fig. 8.

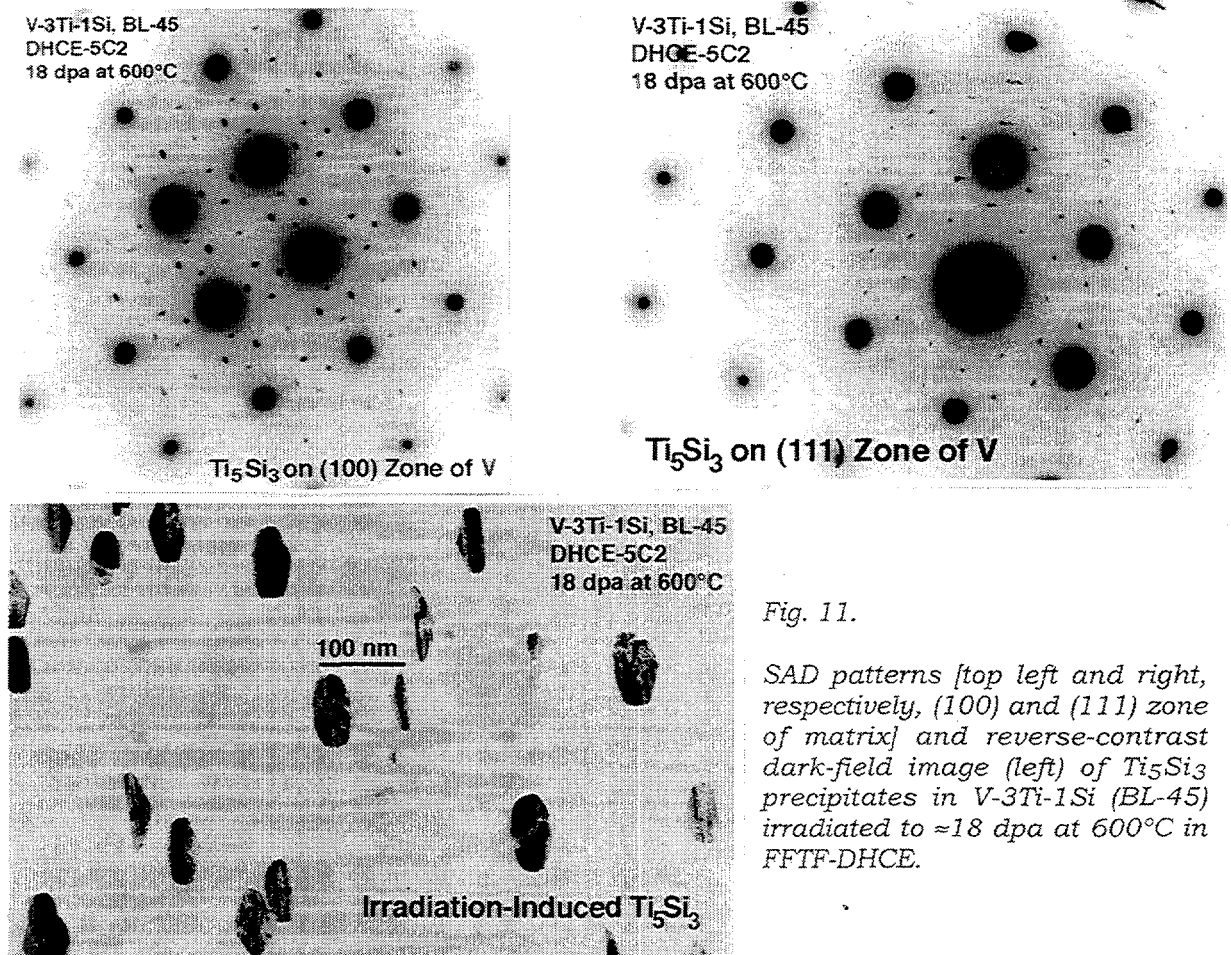


Fig. 11.

SAD patterns [top left and right, respectively, (100) and (111) zone of matrix] and reverse-contrast dark-field image (left) of Ti_5Si_3 precipitates in V-3Ti-1Si (BL-45) irradiated to ≈ 18 dpa at $600^\circ C$ in FFTF-DHCE.

DISCUSSION

For the specimens of the 500-kg V-4Cr-4Ti (Heat 832665) that was irradiated to ≈ 4 dpa at $390^\circ C$ in the EBR-II X530 experiment, the number density of the $(V,Ti_{1-x})(C,O,N)$ precipitates was extremely high, as shown in Fig. 6, whereas irradiation-induced precipitation of other phases in the same specimens, such as Ti_5Si_3 , was negligible. It seems quite possible that irradiation-induced hardening of the material is mostly due to the high-density $(V,Ti_{1-x})(C,O,N)$ precipitates rather than to defect clusters or dislocation loops that act as primary barriers to dislocation motion. In agreement with a previous investigation,¹¹ it was difficult to obtain dark-field images of pure defect clusters (dislocation loops free of precipitate) in TEM disks or tensile specimens of this material, because most precipitate reflections were superimposed on matrix reflections. The size and number density of $(V,Ti_{1-x})(C,O,N)$ precipitates that were visible in dark-field images, and the size and number density of all types of barriers (defect clusters, dislocation loops, and precipitates) that were visible in the bright-field image were similar. This observation indicates that $(V,Ti_{1-x})(C,O,N)$ precipitated on or near most defect clusters and dislocation loops in the material.

From bright-field images (e.g., Fig. 2) alone, we cannot obtain direct evidence that helps clarify the role of the precipitates in dislocation channeling, nor can we gain insight into what alloying or impurity elements are responsible for precipitation-induced microstructural modification. However, the dark-field images (e.g., Fig. 12) provide more direct evidence for the role of $(V,Ti_{1-x})(C,O,N)$ precipitates in dislocation channeling. The dark-field image in Fig. 12 shows that $(V,Ti_{1-x})(C,O,N)$ precipitates, contained in a tensile specimen of the 500-kg V-4Cr-4Ti (Heat 832665) that was irradiated to ≈ 4 dpa at $390^\circ C$ in the EBR-II X530 and tested at

390°C, were either sheared or plowed out of dislocation channels. Therefore, the severe dislocation channeling and poor work-hardening capability (manifested by uniform elongation <0.8%, Fig. 1A) of the material did, indeed, seem to be a direct consequence of extensive irradiation-induced precipitation of $(V,Ti_{1-x})(C,O,N)$ in the material. Likewise, the poor impact property of the material⁷ is believed due to the same precipitation-induced microstructural degradation.

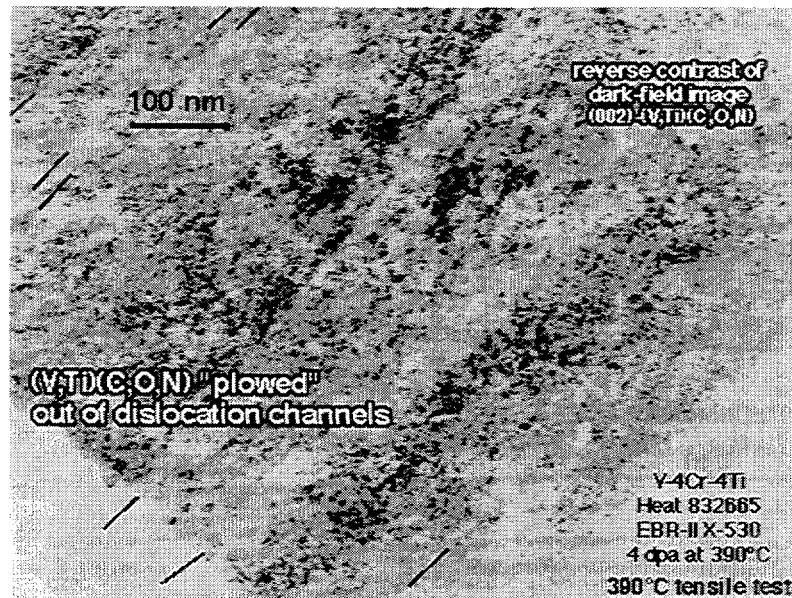


Fig. 12.

Reverse-contrast dark-field image of $(V, Ti_{1-x})(C, O, N)$ precipitates and dislocation channels in 500-kg V-4Cr-4Ti (Heat 832665) irradiated to ≈ 4 dpa at 390°C in EBR-II X530 and tensile tested at 390°C, showing that the precipitates were sheared or plowed out of dislocation channels.

In contrast to the case of the 500-kg heat V-4Cr-4Ti that was irradiated in the EBR-II, uniform elongation (i.e., 1.4–2.0 %) and work-hardening capability of the 30-kg V-4Cr-4Ti heat were relatively higher after irradiation to ≈ 27 dpa at $\approx 430^\circ\text{C}$ in the FFTF-DHCE (see Fig. 1A).⁷ This finding is consistent with the dark-field image of the microstructure of the latter material, shown in Fig. 9. The density of the fine $(V, Ti_{1-x})(C, O, N)$ precipitates produced in the 30-kg heat was more than an order of magnitude lower than that of the 500-kg heat, and as a consequence, the 30-kg heat seems to be more resistant to dislocation channeling, and hence, to flow localization. Similarly, a 15-kg heat of V-3Ti-1Si (BL-45) exhibited no sign of $(V, Ti_{1-x})(C, O, N)$ precipitation after irradiation at 430°C in the FFTF-DHCE or at 390°C in the COBRA-1A2 experiment. This observation is also consistent with the relatively higher work-hardening capability of the BL-45 specimens that is manifested by uniform elongations as high as 3.8–6.5% (see Fig. 1B). Thus, at least for three irradiated materials, i.e., V-4Cr-4Ti Heat 832665 irradiated to ≈ 4 dpa at 390°C in the EBR-II X530, V-4Cr-4Ti Heat BL-47 irradiated to ≈ 27 dpa at 430°C in the FFTF-DHCE, and V-3Ti-1Si Heat BL-45 irradiated to ≈ 27 dpa at 430°C in the FFTF-DHCE, we observed direct evidence for good correlation among the number density of the fine $(V, Ti_{1-x})(C, O, N)$ precipitates, the degree of dislocation channeling, and work-hardening capability.

Obviously, one way to improve work-hardening capability (and, at the same time, impact properties) of V-base alloys that are to be irradiated at $<430^\circ\text{C}$ is to suppress or prevent irradiation-induced precipitation of $(V, Ti_{1-x})(C, O, N)$. As shown in Fig. 1A, the coldworked specimen of BL-47 V-4Cr-4Ti exhibited better work-hardening capability than the annealed material (i.e., uniform elongation ≈ 2.3 vs. 0.9% after irradiation at 390°C), indicating that coldwork improves work-hardening capability. However, optimizing alloy or specimen fabrication procedures, such as coldworking, keeping C, O, and N concentrations at a sufficiently low level, or maximizing thermal precipitation, is probably either insufficient, too costly, or impractical. Alternatively, it may be feasible, by adding certain doping element(s), to shift the range of temperature of irradiation-induced $(V, Ti_{1-x})(C, O, N)$ precipitation to

sufficiently lower temperatures, e.g., $<350^{\circ}\text{C}$, or even entirely eliminate precipitation in the temperature range of interest for fusion application.

Doping V-4Cr-4Ti with $>1\%$ Si appears to be an attractive idea. As shown in Fig. 1B, the work-hardening capability of BL-27 V-3Ti-0.25Si was significantly inferior to that of BL-45 V-3Ti-1Si. Although not conclusive at this time, this difference in work-hardening capability may be a manifestation of a beneficial effect of sufficiently high Si concentration in V-3Ti-Si alloys; e.g., $(\text{V},\text{Ti}_{1-x})(\text{C},\text{O},\text{N})$ precipitation and dislocation channeling is suppressed in the high-Si heat but is still active in the low-Si heat. Likewise, a sufficiently high Si concentration could also help to suppress or prevent $(\text{V},\text{Ti}_{1-x})(\text{C},\text{O},\text{N})$ precipitation in V-4Cr-4Ti at temperatures $<450^{\circ}\text{C}$.

CONCLUSIONS

1. Dislocation channeling and poor work-hardening capability of the 500-kg heat of V-4Cr-4Ti, observed after irradiation at low temperatures (e.g., at $<400^{\circ}\text{C}$), are caused by high-density irradiation-induced precipitation of very fine $<10\text{-nm}$ particles. By dark-field imaging and selected area diffraction analysis, the characteristic precipitates were identified as $(\text{V},\text{Ti}_{1-x})(\text{C},\text{O},\text{N})$, which has an fcc structure and modified composition of VC, with some V replaced by Ti and some C replaced by O, and, to a lesser extent, by N. The same type of precipitates were also observed in unalloyed V, V-5Ti, V3Ti-1Si, and a 30-kg heat of V-4Cr-4Ti irradiated at $430\text{--}600^{\circ}\text{C}$ in the dynamic helium charging experiment; precipitation behavior was influenced strongly by irradiation temperature.
2. Irradiation-induced precipitates of $(\text{V},\text{Ti}_{1-x})(\text{C},\text{O},\text{N})$ exhibited two orientations: $(111)_{\text{V}(\text{C},\text{O},\text{N})} // (110)_{\text{V}}$, $[0-22]_{\text{V}(\text{C},\text{O},\text{N})} // [002]_{\text{V}}$; and $(100)_{\text{V}(\text{C},\text{O},\text{N})} // (100)_{\text{V}}$, $[002]_{\text{V}(\text{C},\text{O},\text{N})} // [011]_{\text{V}}$. Diffraction spots from the $<10\text{-nm}$ $(\text{V},\text{Ti}_{1-x})(\text{C},\text{O},\text{N})$ precipitates in the 500-kg V-4Cr-4Ti, irradiated to ≈ 4 dpa at 390°C , exhibited streaks in the $<110>$ and $<111>$ directions, indicating that they are very fine needlelike precipitates. In contrast, relatively large $(\text{V},\text{Ti}_{1-x})(\text{C},\text{O},\text{N})$ precipitates produced during irradiation at 600°C exhibited streaks in the $<110>$ direction only, showing that they are thin platelets (≈ 10 nm thick and $50\text{--}120$ nm in diameter). Thermally formed platelet $(\text{V},\text{Ti}_{1-x})(\text{C},\text{O},\text{N})$ precipitates were also observed in unirradiated postwelding-annealed laser and electron-beam welds of the 500-kg V-4Cr-4Ti.
3. In V-4Cr-4Ti at <27 dpa, $(\text{V},\text{Ti}_{1-x})(\text{C},\text{O},\text{N})$ precipitation is predominant for irradiation at $<430^{\circ}\text{C}$, whereas Ti_5Si_3 precipitation is favored at $>500^{\circ}\text{C}$.
4. Dark-field images provided direct evidence that $(\text{V},\text{Ti}_{1-x})(\text{C},\text{O},\text{N})$ precipitates in tensile specimens of the 500-kg V-4Cr-4Ti (Heat 832665) that were irradiated and tested at 390°C were either sheared or plowed out of dislocation channels. The severe dislocation channeling and poor work-hardening capability of the material is a direct consequence of extensive irradiation-induced precipitation of $(\text{V},\text{Ti}_{1-x})(\text{C},\text{O},\text{N})$. The poor impact property of the heat observed after irradiation at $<390^{\circ}\text{C}$ is probably also due to the same precipitation-induced microstructural degradation.
5. The number density of $(\text{V},\text{Ti}_{1-x})(\text{C},\text{O},\text{N})$ precipitates in the 30-kg heat V-4Cr-4Ti, irradiated to ≈ 27 dpa at $\approx 430^{\circ}\text{C}$ in the dynamic helium charging experiment, was more than an order of magnitude lower than that of the 500-kg V-4Cr-4Ti heat that was irradiated at 390°C in a conventional experiment, and as a consequence, the heat was more resistant to dislocation channeling, and work-hardening capability was higher.
6. A 15-kg heat of V-3Ti-1Si showed no sign of $(\text{V},\text{Ti}_{1-x})(\text{C},\text{O},\text{N})$ precipitation after irradiation at $<430^{\circ}\text{C}$ in either conventional or dynamic helium charging experiments, indicating that the heat is inherently resistant to dislocation channeling. This finding is consistent with high work-hardening capability (uniform elongation of $3.8\text{--}6.5\%$ at <27 dpa) that was observed for the alloy.

7. The work-hardening capability and impact properties of V-base alloys irradiated at $<430^{\circ}\text{C}$ can be improved by preventing irradiation-induced precipitation of $(\text{V},\text{Ti}_{1-x})(\text{C},\text{O},\text{N})$. Optimizing alloy or specimen fabrication procedures, e.g., coldworking, keeping C, O, and N concentrations sufficiently low, or maximizing thermal precipitation, is probably either insufficient, too costly, or impractical. Alternatively, it may be feasible to suppress or prevent $(\text{V},\text{Ti}_{1-x})(\text{C},\text{O},\text{N})$ precipitation by adding certain doping element(s). Doping V-4Cr-4Ti with $>1\%$ Si appears to be an attractive idea.

ACKNOWLEDGMENTS

The authors thank L. J. Nowicki for specimen retrieval, hot-cell mechanical testing, and preparation of specimens for microstructural examination.

REFERENCES

1. D. J. Alexander, L. L. Snead, S. J. Zinkle, A. N. Gubbi, A. F. Rowcliffe, and E. E. Bloom, "Effects of Irradiation at Low Temperature on V-4Cr-4Ti," in Fusion Reactor Materials, Semiannual Prog. Rep. DOE/ER-0313/20, Oak Ridge National Laboratory, Oak Ridge, TN (1996), pp. 87-95.
2. H. M. Chung, L. Nowicki, and D. L. Smith, "Tensile Properties of Vanadium Alloys Irradiated at 400°C in the HFIR," in Fusion Reactor Materials, Semiannual Prog. Rep. DOE/ER-0313/20, Oak Ridge National Laboratory, Oak Ridge, TN (1996), pp. 84-86.
3. H. M. Chung, L. Nowicki, and D. L. Smith, "Tensile Properties of Vanadium Alloys Irradiated at 200°C in the HFIR," in Fusion Reactor Materials, Semiannual Prog. Rep. DOE/ER-0313/22, Oak Ridge National Laboratory, Oak Ridge, TN (1997), pp. 29-32.
4. S. J. Zinkle, D. J. Alexander, J. P. Robertson, L. L. Snead, A. F. Rowcliffe, L. T. Gibson, W. S. Eatherly, and H.-C. Tsai, "Effect of Fast Neutron Irradiation to 4 dpa at 400°C on the Properties of V-(4-5)Cr-(4-5)Ti Alloys," in Fusion Reactor Materials, Semiannual Prog. Rep. DOE/ER-0313/21, Oak Ridge National Laboratory, Oak Ridge, TN (1997), pp. 73-78.
5. H. M. Chung, H.-C. Tsai, L. J. Nowicki, and D. L. Smith, "Tensile Properties of Vanadium Alloys Irradiated in EBR-II," in Fusion Reactor Materials, Semiannual Prog. Rep. DOE/ER-0313/22, Oak Ridge National Laboratory, Oak Ridge, TN (1997), pp. 18-21.
6. H.-C. Tsai, L. J. Nowicki, M. C. Billone, H. M. Chung, and D. L. Smith, "Tensile and Impact Properties of Vanadium Alloys Irradiated at Low Temperatures in the ATR-A1 Experiment," in Fusion Reactor Materials, Semiannual Prog. Rep. DOE/ER-0313/23, Oak Ridge National Laboratory, Oak Ridge, TN (1998), pp. 70-76.
7. H. M. Chung and D. L. Smith, "Tensile and Impact Properties of Vanadium Alloys Irradiated at $<430^{\circ}\text{C}$," *J. Nucl. Mater.*, 1998, (Proc. 8th Intl. Conf. Fusion Reactor Materials, Oct. 26-31, 1997, Sendai, Japan), in press.
8. H. M. Chung, B. A. Loomis, and D. L. Smith, *J. Nucl. Mater.* 239 (1996) 139.
9. B. A. Loomis, H. M. Chung, L. Nowicki, and D. L. Smith, *J. Nucl. Mater.* 212-215 (1994) 799-803.
10. J. Gazda, M. Meshii, and H. M. Chung, "Microstructure of V-4Cr-4Ti Alloy After Low Temperature Irradiation by Ions and Neutrons," *J. Nucl. Mater.*, 1998, (Proc. 8th Intl. Conf. Fusion Reactor Materials, Oct. 26-31, 1997, Sendai, Japan), in press.
11. D. S. Gelles, P. M. Rice, S. J. Zinkle, and H. M. Chung, "Microstructural Examination of Irradiated V-4Cr-4Ti," *ibid.*
12. P. M. Price and S. J. Zinkle "Temperature Dependence of the Radiation-Damage Microstructure in V-4Cr-4Ti Neutron-Irradiated to Low Dose," *ibid.*

13. H. M. Chung, M. C. Billone, and D. L. Smith, "Effect of Helium on Tensile Properties of Vanadium Alloys," in Fusion Reactor Materials, Semiannual Prog. Rep. DOE/ER-0313/22, Oak Ridge National Laboratory, Oak Ridge, TN (1997), pp. 22-28.
14. B. S. Hickman, *J. Inst. Met.* 96 (1968) 330-337.
15. Ch. Leibovich, A. Rabinkin, and M. Talikaner, *Met. Trans. A12* (1981) 1513-1519.
16. M. Hansen, *Constitution of Binary Alloys*, McGraw-Hill Book Co., 2nd Ed., New York, 1958.
17. F. A. Shunk, *Constitution of Binary Alloys, 2nd Supplement*, McGraw-Hill Book Co., New York, 1969.
18. H. M. Chung, J.-H. Park, R. V. Strain, K. H. Leong, and D. L. Smith, "Mechanical Properties and Microstructural Characteristics of Laser and Electron-Beam Welds in V-4Cr-4Ti Alloy After Low Temperature Irradiation by Ions and Neutrons," *J. Nucl. Mater.*, 1998, (Proc. 8th Intl. Conf. Fusion Reactor Materials, Oct. 26-31, 1997, Sendai, Japan), in press.
19. V. Kazakov, V. Chakin, and Z. Ostrovsky, *J. Nucl. Mater.* 233-237 (1996) 364.
20. H. M. Chung, B. A. Loomis, and D. L. Smith, *ASTM STP-1175* (1993) 1185.